

## PROTOTYPE OF A DSP-BASED INSTRUMENT FOR IN-SERVICE WIRELESS TRANSMITTER POWER MEASUREMENT

Leopoldo Angrisani<sup>1)</sup>, Felice Cennamo<sup>1)</sup>, Giovanni Scarpato<sup>2),3)</sup>, Rosario Schiano Lo Moriello<sup>1)</sup>

1) University of Naples Federico II, Dept. of Electrical Engineering and Information Technologies, via Claudio 21 – 80125 Naples, Italy, ({angrisan; cennamo; rschiano}@unina.it)

2) University of Naples “Parthenope”, Department. of Engineering, Centro Direzionale di Napoli Isola C4 – 80143 Naples, Italy, (giovanni.scarpato@uniparthenope.it)

3) Osservatorio Vesuviano, Istituto Nazionale di Geofisica e Vulcanologia Via Diocleziano, 328 – 80124 Naples, Italy, (giovanni.scarpato@ingv.ov.it)

### Abstract

A prototype of a DSP-based instrument for in-service transmitter power measurements is presented. The instrument implements a signal-selective algorithm for power measurements that is suitable for use in wireless environments, where possible uncontrolled interfering sources are present in the radio channel and are overlapped to the signal emitted by the transmitter under test, possibly in both time and frequency domain. The measurement method exploits the principles of cyclic spectral analysis, which are briefly recalled in the paper. Potentialities, as well as limitations of the prototype use are discussed, and the results of experiments with both modulated and unmodulated interfering sources are presented.

Keywords: wireless transmitters, power measurements, in-service testing, DSP.

© 2014 Polish Academy of Sciences. All rights reserved

### 1. Introduction

In-service testing of wireless transmitters is a part of the transmitting systems reliability assessment [1–4]. In-service transmitter testing is usually performed in the frequency domain and is potentially subject to the effects of interfering signals occupying the same channel or adjacent channels [5–6]. The problem is even more severe with regard to opportunistic systems that use the Dynamic Spectrum Access (DSA), where the secondary user would temporarily occupy the spectrum unutilized by the primary user [7–8]. One of the key and easiest parameters that is measured during in-service transmitter testing is the signal power. Also, as highly integrated wireless communication circuits are often based on the quadrature modulation, the radiofrequency (RF) transmitter diagnostics is often based on I/Q impairment measurements, typically through loop-back tests [9–10] or received signal processing [11–16].

However, along with the well-known repeatability problems that power measurements of radiofrequency signals can suffer from [17–18], the power measurements can actually become challenging when the interfering signal(s) and useful signal overlap in time and frequency, especially in the case of a low signal-to-noise (SNR) ratio [19–25].

An innovative method to reliably measure the signal power in presence of a co-channel interference was presented in [26]. The method is based on a signal-selective algorithm that exploits the cyclic spectral analysis [27] to measure the power of the sole desired signal, discarding interference. The cyclostationarity-based method exhibits a good performance and

succeeds in reliably measuring the desired signal power, even in cases when a simple spectral analysis fails in separating desired and interfering signals.

This paper is an extended version of the paper [28], and describes the prototype of a DSP-based instrument originally presented in [21] that, based on the aforementioned method, permits to perform in-service power measurements of wireless transmitters, even in unlicensed bands, where the risk of meeting an uncontrolled interference is not negligible. In the following, after some basics on cyclostationarity and theoretical information on the measurement principle, the prototype implementation is described and the results of some experiments are presented.

## 2. Wireless power measurements under interference

In this section, the proposed measurement method for in-service transmitter power measurements, which is suitable to operate in (critical) noise and interference conditions is presented. As the method is based on the cyclic spectral analysis of the noisy signal, some notes on cyclostationarity are first given, for the sake of readability. Then, details of the measurement method are provided, along with a presentation of the cyclic spectral characteristics of the most common modulation formats which are needed to implement the method.

### 2.1. General aspects of the cyclic spectral analysis

A continuous-time real-valued stochastic process  $x(t)$  is said to be almost-cyclostationary (ACS) in a wide sense if its autocorrelation function  $R_x(t, \tau)$  is an almost periodic function of  $t$ . In such a case,  $R_x(t, \tau)$  can be expressed as the limit of a uniformly convergent sequence of trigonometric polynomials in  $t$ :

$$R_x(t, \tau) = \sum_{\alpha \in A} R_x^\alpha(\tau) e^{j2\pi\alpha t}. \quad (1)$$

The coefficients of the sequence,  $R_x^\alpha(\tau)$ , are named *the cyclic autocorrelation functions*, whereas  $\alpha$  are *the cycle frequencies*. The vast majority of communication signals are ACS, as a consequence of a periodicity of some kind, connected with such operations, as e.g. coding, modulation or sampling. Their cycle frequencies are thus usually associated with typical parameters, such as the baud rate, sample rate and carrier frequency. When the autocorrelation function  $R_x(t, \tau)$  is a periodic function of  $t$  (e.g. with a period  $T$ ), the set  $A$  contains cycle frequencies that are all multiples of the fundamental one (i.e.  $A \equiv \left\{ \frac{n}{T} \right\}_{n \in \mathbb{Z}}$ ), and the process  $x(t)$  is said to be cyclostationary in a wide sense.

A second-order characterization of ACS processes in the frequency domain can be easily obtained from (1):

$$E\{X(f_1)X^*(f_2)\} = \sum_{\alpha \in A} S_x^\alpha(f) \delta(f_2 - f_1 + \alpha), \quad (2)$$

where  $X(f)$  is the Fourier transformation of  $x(t)$ , which is assumed to exist at least in the sense of distributions (generalized functions), with probability 1,  $\delta(\cdot)$  is the Dirac delta, the superscript  $*$  is the symbol of the operation of complex conjugation, and

$$S_x^\alpha(f) \triangleq \int_{\mathbb{R}} R_x^\alpha(\tau) e^{-j2\pi f \tau} dt, \quad (3)$$

is usually referred to as either the *cyclic spectrum* at the cycle frequency  $\alpha$  or the *spectral correlation density function*.

Special care must be put when exploiting cyclic spectral analysis results to sampled signals. Indeed, it can be shown that the sampled version of a continuous-time almost-cyclostationary signal is a discrete-time almost-cyclostationary signal, whose cyclic spectra are related to those of the continuous-time signal [29]. However, aliasing can occur in the cyclic spectral domain, just as it can happen in the frequency domain. In this case, the avoidance of aliasing is granted by the choice of a sampling frequency that is as high as at least four times the bandwidth of  $x(t)$ , assuming  $x(t)$  is a strictly band-limited process. A thorough and comprehensive treatment of cyclostationarity can be found in [27] and references therein.

## 2.2. Power measurement

The measurement method implemented in the proposed DSP-based instrument was originally presented in [26]. It is based on a signal-selective algorithm that exploits the possibility of achieving signal separation in the cyclic spectral domain, even when in both the time and frequency domains the signal and interference (plus noise) completely overlap each other. The basic idea is to extract the cyclic spectra of the original signal by processing the samples of the combination of signal and interference, and then to measure the signal power thanks to a straightforward analytical relation between the cyclic spectra and power. This is possible only if the analysis is conducted at a cycle frequency that is exhibited by the signal but not by interference. Please note that such assumption is not too limiting, as the condition under which the signal and interference have coincident sets  $A$  (see equation (1)) is extremely rare.

Assuming the received signal  $v(t)$  is the sum of the signal  $x(t)$  and interference  $y(t)$ , if  $x(t)$  and  $y(t)$  are zero-mean and uncorrelated, it holds

$$S_v^\alpha(f) = S_x^\alpha(f) + S_y^\alpha(f). \quad (4)$$

So, if the analysis is conducted for a value of  $\alpha$  that is not a cycle frequency of the interference  $y(t)$ , which means  $S_y^\alpha(f) = 0$ , the equation (4) reduces to

$$S_v^\alpha(f) = S_x^\alpha(f), \quad (5)$$

and the cyclic spectrum  $S_x^\alpha(f)$  can thus be easily estimated from  $v(t)$ .

Now, considering a modulated signal  $x(t)$

$$x(t) = s(t) \cos(2\pi f_c t + \varphi_0), \quad (6)$$

where  $s(t)$  is a pulse amplitude modulation (PAM) signal with a wide-sense stationary and white modulating sequence, it can be shown [26] that  $x(t)$  is ACS and its cycle frequencies are  $\left\{\frac{k}{T_0}\right\}$  and  $\left\{\pm 2f_c + \frac{k}{T_0}\right\}$ ,  $k \in \mathbf{Z}$ .

If  $x(t)$  is rewritten as  $A x_1(t)$ , where  $x_1(t)$  is a unitary power signal, then from (5), the power of the signal  $x(t)$ , i.e.  $A^2$ , could in principle be calculated as

$$A^2 = \frac{|S_v^\alpha(f)|}{|S_{x_1}^\alpha(f)|}, \quad (7)$$

where the cyclic spectrum of  $x_1(t)$  depends on the transmitter and can be assumed to be known, since the cyclic spectra of the most common modulated signals are known [30].

Actually, in order to reduce measurement uncertainty, the proposed instrument measures the power of  $x(t)$  through integration of (5) in the frequency variable  $f$ , as

$$A^2 = \frac{\int_{-\infty}^{+\infty} |S_v^\alpha(f)| df}{\int_{-\infty}^{+\infty} |S_{x_1}^\alpha(f)| df}. \quad (8)$$

### 3. Prototype of the instrument

The prototype of the instrument is shown in Fig. 1. It consists of an external 14-bit analog-to-digital converter (ADC) AD9244, characterized by 65 MS/s maximum sampling frequency, an extender that allows interconnection between the ADC and the digital signal processing unit, and an ADSP-21364 Sharc processor, mounted on a compatible development board by Analog Devices (EZKIT).

The ADSP Sharc processor is specifically addressed to real-time applications, and proves itself suitable and reliable for the implementation of embedded measurement devices in different application areas [31–33]. In its architecture, three fundamental parts can be singled out: the core processor, the memory block and the I/O processor. The core processor has two computational units and a cache memory to store frequently occurring instructions. Each computational unit has its own multiplier, ALU, shifter and data register file. The computational units are able to execute for each cycle a sum, a multiplication and a dual data fetch. The system is able to operate in the SIMD (single instruction multiple data) mode, when both computational units are used simultaneously. The memory access and data transfer are performed through the dedicated I/O processor, different from the core processor.

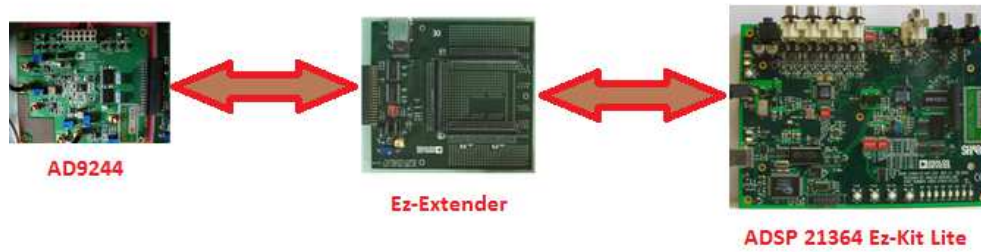


Fig. 1. Instrument prototype.

When a new power measurement is to be made, a boot thread is started to initialize the process. Specifically, it unmask an interrupt request to give start to the data transfer from the ADC to the memory buffer of the processor.

After the digitization, which exploits all the memory depth, the samples are processed to estimate the cyclic autocorrelation function, which could in principle be calculated as

$$R_{xy}(m) = \begin{cases} \frac{1}{N} \sum_{n=0}^{N-m-1} x_{n+m} y_n^*, & m \geq 0 \\ R_{xy}^*(-m), & m < 0 \end{cases} \quad (9)$$

where  $x_n = x(n T_s)$ ,  $T_s = 1/f_s$  being the sampling period, and  $y = x e^{-j2\pi\alpha t}$ . Actually, the vector  $y$  is memorized as a global variable, to avoid a time-consuming recalculation for each value of  $m$ , and to comply with the memory limitation for local variables. The sum in (9) is calculated by exploiting the additive property, i.e. in four successive steps. Moreover, the operations are directly performed on the real and imaginary parts of the numbers in (9) in order to minimize the call to nested functions. Furthermore, to reduce the computational burden and consequently the measurement time, the autocorrelation is windowed, i.e. it is calculated only for the most relevant values of  $m$ .

Subsequently, the fast Fourier transform (FFT) algorithm is applied to the autocorrelation in order to straightforwardly estimate the cyclic spectrum. This is the reason why the autocorrelation is calculated on a number of points equal to a power of 2.

Finally, the power measurement is performed by summing the modulus values of the cyclic spectrum and dividing the result by a known scaling factor, i.e. making a discrete calculation of the right-side part of the expression (7).

#### 4. Experiments

Some experiments have been conducted to evaluate the performance of the prototype in emulated conditions, i.e. when interfering signals are digitally synthesized and summed to the samples of the useful signal. In these tests, channel conditions such as multipath and fading have not been taken into account. It is worth noting that the anti-aliasing conditions cited in the previous section, along with the limited sampling frequency of the prototype has forced to take into consideration signals at relatively low frequencies.

The measurement station is shown in Figure 2. It includes a 14-bit arbitrary waveform generator (AWG) Agilent Technologies E4438C, used to emit the PAM signal as well as the interfering signals, and a digital processing and control unit, i.e. a laptop, which are interconnected through a standard IEEE 488 interface bus. The prototype is connected to the laptop and controlled through a USB cable.

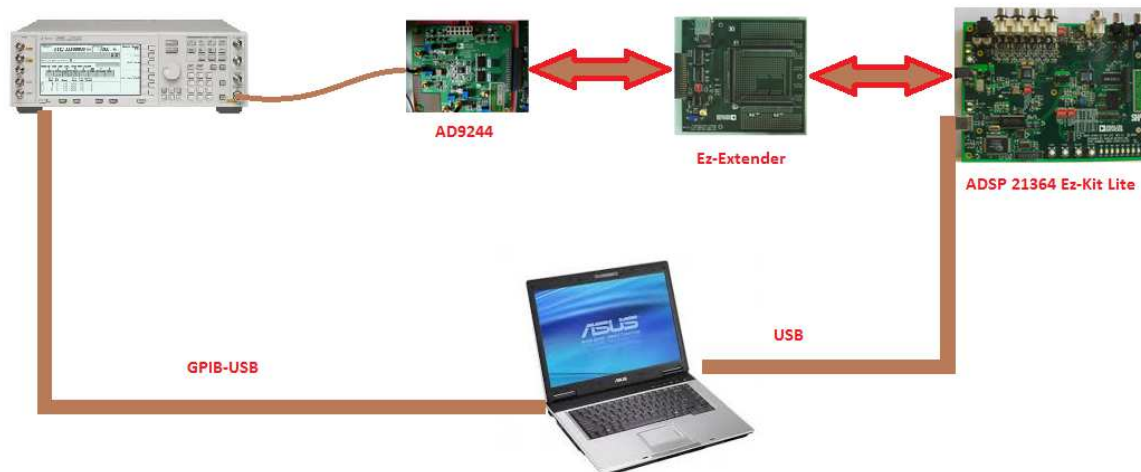


Fig. 2. Measurement station.

To evaluate the quality of the power measurement results, a number of initial tests have been conducted on the sole signal, when no interference is added. In all the tests, the difference between the measured power value and the nominal power value is calculated for different cycle frequencies, and the histogram of the differences is evaluated. This permits to compare the ability of the instrument to extract the power of the useful signal even in critical interference conditions and to compare the repeatability of such measurements to the “intrinsic” repeatability exhibited in absence of interference.

The signal generated for the tests is a binary PAM with the root-raised cosine base pulse, whereas PAM and multi-tone signals have been considered as interfering signals.

Table 1 shows the achieved results, in terms of the average and maximum difference  $\Delta$ , and of the standard deviation  $\sigma$ , over two hundred repeated measurements for each cycle frequency considered, for a PAM signal characterized by the symbol rate  $T = 200 \mu\text{s}$ , and the carrier frequency  $f_c = 10 \text{ MHz}$ . Differences and standard deviations are expressed in percentage relative terms with respect to the nominal power value.

Table 2 and Table 3 show, respectively, the results obtained with multi-tone and different PAM interfering signals, the useful signal being the same. In particular, the multi-tone interference is the superposition of two sinusoids with frequencies 8.5 MHz and 9.5 MHz. It is no surprise that if the measurement is performed at cycle frequencies  $2f_c$  and  $1/T + 2f_c$ , the results are very poor: it happens because the interfering signals exhibit cyclostationarity at frequencies 17 MHz and 19 MHz, which are pretty near  $2f_c$  and  $1/T + 2f_c$ . As stated in the previous section, the analysis has to be carried out at cycle frequencies that are different from the useful signal and the interference. At the same time, results achieved with  $\alpha = 1/T$  are comparable to those obtained without interference.

Regarding interference signals sharing the same modulation format as the useful signal (i.e., PAM), results shown in Table 3 give evidence of the good performance of the method implemented on the prototype, since the values of average percentage difference and standard deviation are generally comparable to those achieved without interference, and reported in Table 1. It can again be noted, that choosing a cycle frequency that is exhibited also by the interfering signal for the analysis leads to very bad results due to the impossibility of separating the cyclic spectra of the useful signal and interference.

Finally, Table 4 shows the results achieved when a PAM signal with symbol period equal to 1 ms and a sinusoidal signal sharing the same carrier frequency  $f_c$  are interfering with the transmitted signal. As expected, the performance is poor when the wrong cycle frequency, i.e.  $\alpha = 2f_c$ , is chosen. However, the results obtained when the signal is analysed at  $\alpha = 1/T$  are very good, and demonstrate how the proposed instrument permits to estimate the power of the transmitted signal with a few percent error, even when the signal is completely overlapped within time and frequency with interference.

Table 1. Measurement results without interference.

Cycle frequency $\alpha$	Average $\Delta$ %	Maximum $\Delta$ %	Relative std. dev. $\sigma$ [%]
$1/T$	0.8	10	2.0
$2f_c$	2.2	7.7	2.4
$1/T + 2f_c$	5.7	13	2.4

Table 2. Measurement results with multitone interference.

Cycle frequency $\alpha$	Average $\Delta$ [%]	Maximum $\Delta$ [%]	Relative std. dev. $\sigma$ [%]
$1/T$	2.8	5.1	2.1
$2f_c$	20	30	7.5
$1/T + 2f_c$	12	16	4.5

Table 3. Measurement results with PAM interference.

Cycle frequency $\alpha$	<i>PAM interference with same T</i>			<i>PAM interference with same <math>f_c</math></i>		
	Average $\Delta \%$	Maximum $\Delta \%$	Relative std. dev. $\sigma$	Average $\Delta \%$	Maximum $\Delta \%$	Relative std. dev. $\sigma$
1/T	95	99	3.4	2.2	6.1	2.2
$2f_c$	3.0	4.2	1.6	83	98	2.7
$1/T + 2f_c$	3.9	5.9	2.8	5.3	10.5	2.5

Table 4. Measurement results with multiple PAM interference.

Cycle frequency $\alpha$	<i>Sum of interfering PAM signal and sinusoidal tone at the same <math>f_c</math></i>		
	Average $\Delta \%$	Maximum $\Delta \%$	Relative std. dev. $\sigma$
1/T	6.3	13.1	5.3
$2f_c$	118	143	7.7
$1/T + 2f_c$	8.1	15.2	6.5

## 5. Conclusions

The paper has presented the prototype of a DSP-based instrument for in-service transmitter power measurements, based on a signal-selective algorithm that exploits the principle of the cyclic spectral analysis. To be used effectively, the method requires the a priori knowledge of the basic parameters of the transmitted signal, such as the modulation format, the symbol rate and the carrier frequency, and requires that the signal emitted by the transmitter under test and possible interfering source do not share at least one cycle frequency.

Although the current version of the prototype suffers from some limitations, mainly connected with the maximum sampling frequency and memory depth, the experimental results at an intermediate frequency are promising and have proven that the proposed method, which was originally presented in [26], exhibits a good performance on real communication signals. Thus, the prototype can be considered as a proof of the concept for possible application to the actual transmitters.

The ongoing research activities are mainly focused on the introduction of a down-conversion section before the digitization, which can make the use of the same DSP prototype feasible for

signals at higher frequencies. An interesting alternative could be the adoption of band-pass strategies like in [34–37], with suitable adaptation to cope with the further constraints that have to be introduced to avoid cyclic aliasing.

## Acknowledgement

The authors are grateful to Dr. Michele Vadursi for his cooperation. This work has been partially funded by the Italian Ministry of University and Research (MIUR) within the PRIN project “Innovative measurements for wireless scenarios under critical interference conditions”.

## References

- [1] Venzi, M., Rossin, S., Michelassi, C., Accillaro, C., Catelani, M., Ciani, L. (2013). Improved FBD and RBD generation for system reliability assessment. In *Proc. of 12th IMEKO TC10 Workshop on Technical Diagnostics: New Perspective in Measurements, Tools and Techniques for Industrial Applications*. Florence, Italy, 266–270.
- [2] Catelani, M., Ciani, L., Luongo, V. (2012). Functional safety assessment: An issue for technical diagnostics. In *Proc. of 20th IMEKO World Congress 2012*. Busan, Republic of Korea, 570–574.
- [3] Catelani, M., Ciani, L., Luongo, V. (2012). A new proposal for the analysis of Safety Instrumented Systems. In *Proc. of IEEE - International Instrumentation and Measurement Technology Conference (I2MTC)*. Graz, Austria, 1612–1616.
- [4] Catelani, M., Ciani, L., Luongo, V. (2010). The FMEDA approach to improve the safety assessment according to the IEC61508. *Microelectronics Reliability*, 50 (9), 9–11.
- [5] Jabbar, M., Rahman, M. (1991). Radio frequency interference of electric motors and associated controls. *IEEE Transactions on Industry Applications*, 27(1), 27–31.
- [6] Agilent Technologies Application Note. (2011). Evaluating Fluorescent Lighting Interference on Passive UHF RFID Systems. Literature number 5990-9090. (2014 January). <http://cp.literature.agilent.com/litweb/pdf/5990-9090EN.pdf>.
- [7] Stanislav, F., Kentaro, I., Hiroshi, H. (2010). IEEE Draft Standard P1900.4a for Architecture and Interfaces for Dynamic Spectrum Access Networks in White Space Frequency Bands: Technical Overview and Feasibility Study. In *Proc. of IEEE 21st International Symposium on Personal, Indoor and Mobile Radio Communications Workshops*. Istanbul, Turkey, 15–20.
- [8] Agilent Technologies Application Note. (2013). Techniques for Precise Interference Measurements in the Field. Literature number 5991-0418EN. (2014 January). <http://cp.literature.agilent.com/litweb/pdf/5991-0418EN.pdf>.
- [9] Erdogan, S. E. (2008). Single-Measurement Diagnostic Test Method for Parametric Faults of I/Q Modulating RF Transceivers. In *Proc. of 26th IEEE VLSI Test Symposium*. San Diego, CA, USA, 209–214.
- [10] Srinivasan, G., Chatterjee, A., Taenzler, F. (2006). Alternate Loopback Diagnostic Tests for Wafer-level Diagnosis of Modern Wireless Transceivers Using Spectral Signatures. In *Proc. of 24th IEEE VLSI Test Symposium*, Berkeley, CA, USA, 1–6.
- [11] Darsena, D. (2007). Successive narrowband interference cancellation for OFDM systems. *IEEE Comm. Lett.*, 11 (1), 73–75.
- [12] Darsena, D., Verde, F. (2008). Successive NBI cancellation using soft decisions for OFDM systems. *IEEE Sig. Proc. Lett.*, 15, 873–876.
- [13] Darsena, D., Gelli G., Melito F., Verde F., Vitiello A. (2013). Impulse noise mitigation for MIMO-OFDM wireless networks with linear equalization. In *Proc. of IEEE Intern. Workshop on Measurements and Networking*, Naples, Italy, 94–99.

- [14] Darsena, D., Gelli, G., Verde, F. (2008). Universal linear precoding for NBI-proof widely linear equalization in MC systems. *Eurasip Journal on Wireless Communications and Networking*.
- [15] Angrisani, L., D'Arco, M., Vadursi, M. (2005). Error Vector-Based Measurement Procedures for RF Digital Transmitters Troubleshooting. *IEEE Trans. on Instr. and Meas.*, 54 (4), 1381–1387.
- [16] Darsena, D., Gelli, G., Verde, F. (2014). Perfect symbol recovery and NBI suppression in MIMO-OFDM systems. *Electronics Letters*, 50 (3), 225–227.
- [17] Macii, D., Petri, D. (2007). An effective power consumption measurement procedure for bluetooth wireless modules. *IEEE Trans. on Instrum. and Meas.* 56 (4), 1355–1364.
- [18] Angrisani, L., D'Apuzzo, M., Vadursi, M. (2006). Power Measurement in Digital Wireless Communication Systems through Parametric Spectral Estimation. *IEEE Trans. on Instrum. and Meas.*, 55 (4), 1051–1058.
- [19] Tancredi, U., Renga, A., Grassi, M. (2011). Ionospheric path delay models for spaceborne GPS receivers flying in formation with large baselines. *Advances in Space Research*. 48 (3), 507–520.
- [20] Tancredi, U., Renga, A., Grassi, M. (2013). Validation on flight data of a closed-loop approach for GPS-based relative navigation of LEO satellites. *Acta Astronautica*, 86, 126–135.
- [21] Angrisani, L., Schiano Lo Moriello, R., Vadursi, M. (2008). A New Instrument Based on Cyclic Spectral Analysis for Power Measurement in Digital Telecommunication Systems. In *Proc. of IEEE I2MTC 2008, Intern. Instrum. and Measur. Technol. Conf.*, Victoria, BC, Canada, 1334–1339.
- [22] Angrisani, L., Capriglione, D., Ferrigno, L., Miele, G. (2011). A New Digital Signal Processing Method for Spectrum Interference Monitoring. *Measurement Science Review*, 11 (1), 1–8.
- [23] Betta, G., Capriglione, D., Landi, C., Pasquino, N. (2009). Uncertainty and reproducibility in measuring the data acquisition system immunity to conducted disturbances. *Measurement Science and Technology*, 20 (5).
- [24] Mariscotti, A., Marrese, A., Pasquino, N., Bifulco, P., Liccardo, A., Schiano Lo Moriello, R. (2013). Wide-band and narrow-band characterization of the propagation channel in trains. *International Review of Electrical Engineering (IREE)*, 8 (5), 1467–1472.
- [25] Bondavalli, A., Ceccarelli, A., Gogaj, F., Seminatore, A., Vadursi, M. (2013). Experimental assessment of low-cost GPS-based localization in railway worksite-like scenarios. *Measurement*, 46 (1), 456–466.
- [26] Angrisani, L., Napolitano, A., Vadursi, M. (2009). True-Power Measurement in Digital Communication Systems Affected by In-Channel Interference. *IEEE Trans. on Instrumentation and Measurement*, 58 (12), 3985–3994.
- [27] Gardner, W. A., Napolitano, A., Paura, L. (2006). Cyclostationarity: Half a century of research. *Signal Processing*, 86 (4), 639–697.
- [28] Angrisani, L., Schiano Lo Moriello, R., Scarpato, G., Vadursi, M. (2013). A DSP-Based Instrument for In-Service Wireless Transmitter Power Measurement. In *Proc. of 12th IMEKO TC10 Workshop on Technical Diagnostics: New Perspective in Measurements, Tools and Techniques for Industrial Applications*. Florence, Italy, 208–213.
- [29] Napolitano, A. (1995). Cyclic higher-order statistics: Input/output relations for discrete- and continuous-time MIMO linear almost-periodically time-variant systems. *Signal Processing*, 42 (2), 147–166.
- [30] Gardner, W. A. (1987). Spectral correlation of modulated signals, Part I - Analog modulation. *IEEE Trans. on Communications*, 35 (6), 584–594.
- [31] Baccigalupi, A., Liccardo, A., Grimaldi, D., Carni, D. L. (2011). Digital to analog converters test based on time to voltage conversion. In *Proc. of Instrum. and Meas. Tech. Conf.*, Hangzhou, China, 6–11.
- [32] Angrisani, L., D'Arco, M., Greenhall, C., Schiano Lo Moriello, R. (2008). A digital signal processing instrument for real time phase noise measurements. *IEEE Trans. on Instr. and Meas.*, 57 (10), 2098–2107.
- [33] Melillo, P., Santoro, D., Vadursi, M. (2014). Detection and Compensation of Inter-Channel Time Offsets in Indirect Fetal ECG Sensing. *IEEE Sensors Journal*, 14 (7), 2327–2334.
- [34] Angrisani, L., Vadursi, M. (2008). On the optimal sampling of bandpass measurement signals through data acquisition systems. *Meas. Sci. Technol.*, 10, 1–9.

- [35] Angrisani, L., Capriglione, D., Ferrigno, L., Miele, G. (2009). Bandpass sampling for a new cost effective DVB-T power meter. In *Proc. of IEEE Instrumentation and Measurement Technology Conference, 2009*. Singapore, 1467–1472.
- [36] Angrisani, L., D'Arco, M., Ianniello, G., Vadursi, M. (2012). An Efficient Pre-Processing Scheme to Enhance Resolution in Band-Pass Signals Acquisition. *IEEE Trans. on Instrum. and Meas.*, vol. 61 (11), 2932–2940.
- [37] D'Arco, M., Genovese, M., Napoli, E., Vadursi, M. (2014). Design and Implementation of a Preprocessing Circuit for Bandpass Signals Acquisition. *IEEE Trans. on Instrum. and Meas.*, 63 (2), 287–294.